e-ISSN 2581-0405
Asian Journal of Applied Research for Community Development and Empowerment
Journal home page: http://ajarcde-safe-network.org ISSN 2581-0405

Synthesis of Hydroxyapatite from Snail Shells Using the Precipitation Method

Rahel Aditya Amara Putri [1], Moh Rifqi Maulana[1,], Erwan Adi Saputro[1], Caecillia Pujiastuti[1], Ni Ketut Sari [1]*

[1] *Department of Chemical Engineering, Universitas Pembangunan Nasional "Veteran" Jawa Timur, Surabaya 60294, Indonesia.*

ARTICLE INFO

Article History:
Received: 01 May 2026
Final Revision: 06 May 2026
Accepted: 20 May 2026
Online Publication: 21 May 2026

KEYWORDS

Hydroxyapatite, snail shell, pila ampullacea, precipitation method, calcium carbonate.

CORRESPONDING AUTHOR

*E-mail: 22031010017@student.upnjatim.ac.id

A B S T R A C T

Hydroxyapatite (HA) is a bioceramic widely used in biomedical applications due to its excellent biocompatibility and bioactivity. This study aims to synthesise hydroxyapatite from rice field snail shells (Pila ampullacea) using the precipitation method and to evaluate the effects of phosphoric acid (H_3PO_4) concentration and heating time on the synthesised hydroxyapatite's characteristics. The synthesis was conducted by varying H_3PO_4 concentration from 0.25 to 2 M and heating time from 1 to 3 hours at a calcination temperature of 800°C. The resulting hydroxyapatite was characterized by SEM-EDX, XRF, XRD, and FTIR analyses, and the Ca/P ratio was optimized using Response Surface Methodology (RSM). SEM-EDX analysis revealed porous and agglomerated surface morphology, indicating successful thermal decomposition of calcium carbonate into calcium oxide precursor. XRF results showed that increasing H_3PO_4 concentration and heating time significantly reduced the Ca/P ratio toward the stoichiometric value of hydroxyapatite (1.67), with optimum conditions achieved at 1.5–2 M H_3PO_4 and 2–2.5 hours heating time. XRD analysis confirmed the formation of crystalline hydroxyapatite with an average crystal size of 14.62 nm and crystallinity degree of 81.23%. FTIR spectra identified characteristic phosphate functional groups, confirming hydroxyapatite formation. The RSM optimization demonstrated that both H_3PO_4 concentration and heating time significantly influence the Ca/P ratio. These findings indicate that rice field snail shells have strong potential as a sustainable and cost-effective alternative calcium source for hydroxyapatite synthesis in biomaterial applications.

Contribution to Sustainable Development Goals (SDGs):
SDG 3: Good Health and Well-Being
SDG 9: Industry, Innovation, and Infrastructure
SDG 12: Responsible Consumption and Production

1. INTRODUCTION

1.1. Research Background

Hydroxyapatite (HA) is a bioceramic material that has structural and compositional similarities to the mineral constituents of human bones and teeth, resulting in high biocompatibility and bioactivity. This material is widely used in the biomedical field, particularly in dental applications such as filling materials, restorative agents, and hard dental tissue regeneration. The development of HA-based nanocomposites has demonstrated improvements in mechanical properties and the ability to control the release of therapeutic agents [1]. In addition, highly porous HA can support enamel remineralization and dentin repair processes due to its osteoconductive properties [2]. Conventional HA production generally relies on pure chemical precursors, which are relatively expensive and less environmentally friendly. Therefore, the utilization of biomaterial waste as an alternative calcium source has attracted significant attention in the development of sustainable materials. Biological waste, such as animal bones and shells, has been widely used as raw materials for HA synthesis [3]. The shell of the rice field snail (*Pila ampullacea*) is one type of agricultural waste that is rich in calcium carbonate ($CaCO_3$) and has

This work is licensed under a Creative Commons Attribution-NonCommercial-ShareAlike 4.0 International License
Published under licence by SAFE-Network

the potential to be converted into hydroxyapatite. In addition, hydroxyapatite derived from natural biomaterials has been reported to exhibit good bioactive properties and biocompatibility, making it promising for various applications [4]. Hydroxyapatite nanoparticles are known to exhibit promising antibacterial activity, making them potential candidates for further development in biomedical applications, particularly as antimicrobial agents [5].

Various methods have been developed for the synthesis of hydroxyapatite from biogenic sources, including hydrothermal, ultrasound-assisted precipitation, and precipitation methods. The precipitation method is widely used in hydroxyapatite synthesis due to its relatively simple, cost-effective process and its ability to control material characteristics through synthesis parameters such as pH, temperature, and reactant concentration [6]. Hydroxyapatite synthesised by the hydrothermal method exhibits relatively narrow, intense diffraction peaks, indicating a higher degree of crystallinity [7]. Meanwhile, the precipitation method tends to produce broader diffraction peaks, indicating lower crystallinity and smaller crystallite size, which are attributed to the synthesis conditions, resulting in greater structural variation [8]. This indicates the presence of amorphous regions, which make the material's structure less ordered and reduce its degree of crystallinity [9].

Therefore, this study aims to synthesize hydroxyapatite from rice field snail shells using the precipitation method. The synthesis process was carried out by varying the H_3PO_4 concentration (0.25–2 M) and heating time (1–3 hours). The resulting materials were subsequently characterized to evaluate their physical and chemical properties. The novelty of this study lies in the simultaneous investigation of the combined effects of H_3PO_4 concentration and heating time variations, which have rarely been reported in hydroxyapatite synthesis from snail shells. This approach is expected to produce hydroxyapatite with high purity and favorable mechanical properties, while also supporting the development of sustainable waste-based biomaterials.

1.2. Literature Review

Hydroxyapatite, a calcium phosphate compound with the chemical formula $Ca_{10}(PO_4)_6(OH)_2$, is widely used in various fields, particularly in biomedical and environmental applications. During its development, hydroxyapatite has been used not only as an implant material but also as an adsorbent in waste treatment, especially for removing heavy metal ions from solutions. This is attributed to its porous crystal structure, large surface area, and the presence of active functional groups, such as phosphate (PO_4^{3-}) and hydroxyl (OH^-), which can interact with various contaminants. Hydroxyapatite can be obtained from both synthetic and natural sources. Natural sources such as shell and bone waste have become attractive alternatives due to their cost-effectiveness and environmental friendliness. The synthesis of hydroxyapatite is also relatively simple; one method is precipitation, which is widely used because it can produce materials with high purity and a controllable particle size.

I.2.1 Hydroxyapatite

Hydroxyapatite is not only biologically important but also plays a significant role in the development of modern medical technology and biomaterials [10]. This compound is widely applied as a coating material for various parts of the human body due to its biocompatibility. In addition, hydroxyapatite is used in the reconstruction of bones, teeth, facial structures, jaws, and skulls. Beyond the medical field, hydroxyapatite also plays a role in various cosmetic procedures to repair or enhance certain body parts. Furthermore, hydroxyapatite is utilized in the animal feed industry as a large-scale additive. The presence of hydroxyl (OH^-) groups on the surface of hydroxyapatite enables it to form bonds with polymers or biomolecules, giving this material great potential for tissue regeneration, medical implants, and nanotechnology-based therapies [11]. The overall reaction equation can be written as follows:

$$10CaCO_3 + 6H_3PO_4 + 2H_2O \rightarrow Ca_{10}(PO_4)_6(OH)_2 + 10CO_2 + 6H_2O$$

I.2.2 Characteristics and Synthesis of Hydroxyapatite

Its material properties strongly influence its various applications. These characteristics include physical, chemical, and mechanical properties that are interrelated in determining the performance of hydroxyapatite across different fields of application. Physical properties such as density and molecular weight, chemical properties such as the Ca/P ratio and crystal system, and mechanical properties such as compressive strength and elastic modulus are important parameters in evaluating this material. Therefore, a comprehensive understanding of hydroxyapatite's properties is essential to support its optimal utilisation across various applications, as shown in Table 1.

Table 1. Characteristics of Hydroxyapatite

Chemical composition	$Ca_{10}(PO_4)_6(OH)_2$
Ratio Ca/P	1.67
Crystal system	Hexagonal
Young's modulus (GPa)	80-110
Elastic modulus (GPa)	114
Compressive strength	400-900
Flexural strength	115-200
Density (g/cm^3)	3.16
Relative density (%)	95-99.5
Fracture toughness ($MPa \cdot mm^{1/2}$)	0.7-1.2
Hardness (HV)	600
Decomposition temperature (°C)	>1000
Melting point (˚C)	1614
Thermal conductivity (W/cm·K)	0.013
Biocompatibility	High
Bioactive	High
Biodegradation	Low
Cell compatibility	High
Osteoconductivity	High

Based on Table 1, the characteristics of hydroxyapatite are determined not only by its chemical composition but also by the synthesis method employed. Differences in synthesis methods can affect particle size, morphology, and the degree of crystallinity. One of the commonly used methods is the wet method, which involves liquid-phase reactions that produce solids via precipitation. This method is widely preferred because it is simple, does not require complex equipment, and enables control over particle size and morphology. In addition, the wet method can produce hydroxyapatite with low crystallinity,

resulting in an amorphous structure, which makes it widely utilised in medical and industrial applications [12].

1.3. Research Objective

This study aims to synthesize hydroxyapatite (HA) from rice field snail shells (*Pila ampullacea*) using the precipitation method. It also aims to analyze the effect of variations in H_3PO_4 concentration and heating time on the characteristics of the resulting HA. Furthermore, this study seeks to examine the physical and chemical properties of HA through characterization using SEM-EDX, XRD, and FTIR, as well as to analyze the Ca/P ratio based on XRF data with the assistance of the *Response Surface Methodology* (RSM)

2. MATERIALS AND METHODS

The hydroxyapatite synthesis process using the precipitation method was carried out in a 500 mL beaker glass as the reaction vessel. This vessel was equipped with a magnetic stirrer to maintain solution homogeneity throughout the process. In addition, a thermometer was used to monitor the reaction temperature, ensuring it remained within the predetermined range. During the precipitation process, the calcium solution obtained from the calcination of rice field snail shells was reacted with a phosphoric acid (H_3PO_4) solution in a beaker. Throughout the process, the mixture was stirred at a specific speed to promote uniform hydroxyapatite precipitation. The setup of the hydroxyapatite synthesis apparatus used in this study, employing the precipitation method, is shown in Figure 1.

Figure 1. Hydroxyapatite Synthesis Equipment Setup

This study was conducted to synthesize hydroxyapatite from snail shells using the precipitation method. The calcium solution obtained from the calcination of snail shells was initially placed in a 250 mL beaker and dissolved in 200 mL of aquadest at 80 °C for 30 minutes. To accommodate the volume expansion during the reaction, the solution was transferred to a 500 mL beaker as the main reaction vessel. Subsequently, 0.25 M, 0.5 M, 1 M, 1.5 M, and 2 M phosphoric acid (H_3PO_4) solutions were gradually added to the calcium solution while stirring with a magnetic stirrer at 300 rpm to maintain homogeneity of the mixture. During the process, the precipitation reaction was maintained at 50 °C for 1 h, 1.5 h, 2 h, 2.5 h, and 3 h, respectively, until hydroxyapatite precipitate was formed. After the precipitation process was completed, the mixture was left to stand for complete sedimentation. The resulting precipitate was then separated through filtration and subsequently dried to obtain hydroxyapatite powder. The hydroxyapatite product obtained was analyzed to determine its characteristics against the specified parameters.

3. RESULT AND DISCUSSION

3.1. SEM-EDX Analysis

To determine the surface morphology and elemental composition of the synthesized samples, analysis was performed using a Scanning Electron Microscope (SEM) equipped with an Energy-Dispersive X-ray (EDX) detector. This analysis aimed to examine the material's microstructure and identify its constituent elements, both qualitatively and quantitatively. The SEM-EDX test results were subsequently used to evaluate the success of the synthesis process, as shown in Figure 2.

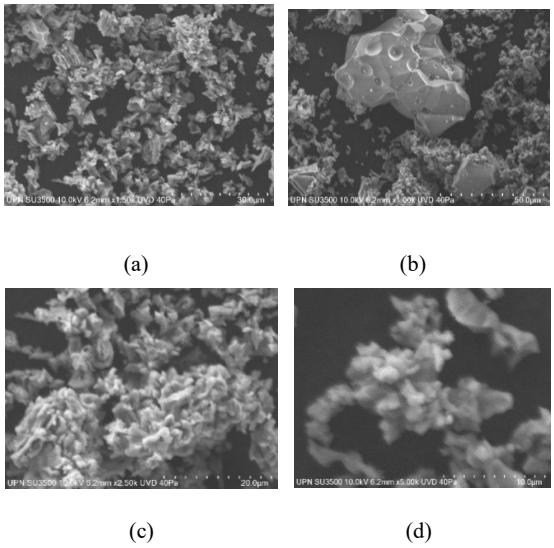

(a) (b)

(c) (d)

Figure 2. SEM-EDX analysis results showing the illustration of porous surface morphology at (a) 1000× magnification, (b) 1500× magnification, (c) 2500× magnification, and (d) 5000× magnification

Based on Figure 2, the SEM-EDX analysis at 10.0 kV indicates that the sample calcined at 800°C exhibits agglomerated particles with irregular shapes. At lower magnifications (1,000×–1,500×), the particle surfaces appeared to contain pores or depressions. Meanwhile, at higher magnifications (2,500×–5,000×), the agglomerates were observed to consist of small particles in the micrometer size range. In general, the material surface appeared rough and porous. This condition occurred due to the release of CO_2 gas during calcination, which formed cavities within the material.

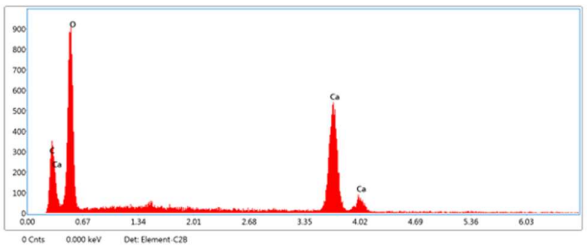

Figure 3. Graph of EDX Analysis Spectrum

Based on the EDX chemical composition analysis shown in Figure 3, the detected elements were predominantly Calcium (Ca) at 55.10% and Oxygen (O) at 44.75%, with Carbon (C) at 0.15%. These data indicate that the calcination process at 800°C predominantly produced calcium oxide (CaO). Comparison with hydroxyapatite (HA) reveals a major difference in the presence of

Phosphorus (P). Hydroxyapatite should contain phosphorus as a constituent element of the phosphate group [13]. However, the absence of P indicates that the sample remained pure CaO, which has the potential to serve as a precursor for hydroxyapatite (HA) synthesis.

3.2 XRF Analysis

Material composition analysis was carried out using X-Ray Fluorescence (XRF) testing at the Integrated Research and Testing Laboratory of Universitas Negeri Malang. This method works by directing X-rays onto the sample surface, thereby exciting the atoms within the sample. The excited atoms then emit fluorescent radiation with characteristic energy or wavelength specific to each element. This radiation is detected by the XRF detector to determine the types and concentrations of elements present in the sample. The analysis results are subsequently presented as elemental ratios to quantitatively describe the material composition, as shown in Table 2.

Table 2. Stoichiometric Data of Ca/P Ratio in Hydroxyapatite under Various Heating Time and H_3PO_4 Concentration Conditions

Calcination Temperature (˚C)	Concentration H_3PO_4 (M)	Time (hours)	Ca (%w/w)	P (%w/w)	Ca/P Ratio
800	0.5	1	73.08	26.1	2.8
	1	1.5	67	31.9	2.1
	1.5	2	62.67	36.6	1.71
	1.5	2.5	62.10	37.15	1.6716
	1.5	3	62.06	37.30	1.6638
	2	1.5	62.33	36.95	1.687
	2	2	62.04	37.45	1.6566
	2	2.5	62.18	37.05	1.6782
	2	3	63.55	35.90	1.77

Based on Table 2, the XRF analysis results indicate that calcination temperature, H_3PO_4 concentration, and reaction time significantly influence the chemical composition of the resulting hydroxyapatite. At a constant temperature of 800 °C, an increase in H_3PO_4 concentration was found to enhance the phosphorus (P) content, thereby reducing the Ca/P ratio. The Ca/P ratio obtained at a concentration of 0.5 M was 2.8, indicating a calcium-rich condition, whereas increasing the concentration up to 1.5 M with a reaction time of 2.5–3 hours resulted in a Ca/P ratio of 1.66–1.67, which is close to the stoichiometric value of hydroxyapatite (1.67). This suggests that the combination of these parameters represents the most optimal synthesis condition in this study. To obtain more accurate optimum conditions, optimization was performed using the Response Surface Methodology (RSM) with the regression equation $y = 4.38309 - 1.5712A - 1.13319B + 0.329822AB + 0.223114A^2 + 0.117164B^2$. This equation indicates the presence of linear, interaction, and quadratic effects of the studied variables on the Ca/P ratio response. The experimental data in Table 2, comprising 9 points, were used to construct this mathematical model.

Furthermore, through the RSM approach, the model was expanded to generate 25 predicted points representing a broader combination of process variables. The resulting model development is presented in Table 3 as optimization data, providing an overview of the relationships among variables and the trend of the response. Thus, Table 3 not only extends the experimental dataset but also clarifies the optimal region of synthesis parameters that yield a Ca/P ratio close to the ideal value for hydroxyapatite.

Table 3. Stoichiometric Data of Ca/P Ratio in Hydroxyapatite under Various H_3PO_4 Concentration and Heating Time Conditions

Calcination Temperature (˚C)	Concentration H_3PO_4 (M)	Time (hours)	Ca/P Ratio
800	0.25	1	3.071
	0.25	1.5	2.692
	0.25	2	2.371
	0.25	2.5	2.110
	0.25	3	1.907
	0.5	1	2.802
	0.5	1.5	2.464
	0.5	2	2.185
	0.5	2.5	1.965
	0.5	3	1.803
	1	1	2.349
	1	1.5	2.094
	1	2	1.897
	1	2.5	1.759
	1	3	1.679
	1.5	1	2.007004
	1.5	1.5	1.83423
	1.5	2	1.720039
	1.5	2.5	1.664429
	1.5	3	1.667402
	2	1	1.776764
	2	1.5	1.686446
	2	2	1.65471
	2	2.5	1.681556
	2	3	1.766984

Based on the data in Table 3, variations in phosphoric acid concentration and reaction time significantly influence changes in the Ca/P ratio, with an increase in solution concentration consistently leading to a decrease in the elemental ratio due to greater availability of phosphate ions in the system. In addition, extending the reaction time is important for stabilising interactions among chemical components until the desired condition is achieved. Overall, the use of higher concentrations combined with longer reaction times has proven effective in directing the formation of a Ca/P ratio close to the ideal stoichiometric value

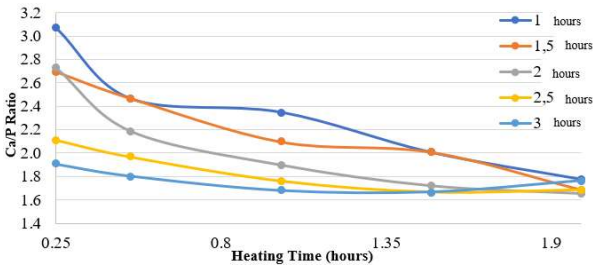

Figure 4. Graph of Heating Time vs. Ca/P Ratio

Based on Figure 4, increasing the reaction time led to a consistent decrease in the Ca/P ratio across all concentration levels. At a concentration of 0.25 M, the ratio decreased sharply

from 3.071 to 1.907, while at 2 M the decrease was more stable, from 1.7768 to 1.767. This indicates that longer reaction times enhance the diffusion of phosphate ions and their binding to calcium, resulting in a material composition closer to the hydroxyapatite standard. The curve, which gradually leveled off at a reaction time of 3 hours, indicates that the system was approaching saturation and the ideal stoichiometric ratio. An adequate calcination duration at 800°C also plays an important role in forming a more mature and stable material structure [14].

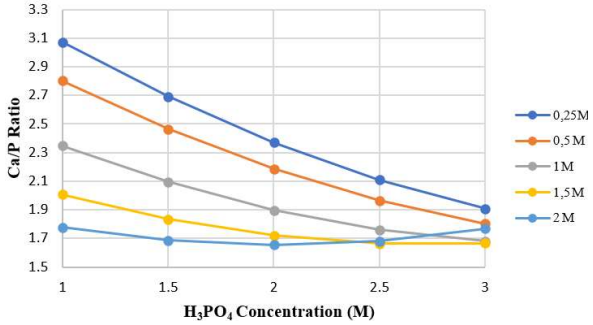

Figure 5. Graph of H_3PO_4 Concentration vs. Ca/P Ratio

Based on Figure 5, increasing the H_3PO_4 concentration significantly decreases the Ca/P ratio. At a concentration of 0.25 M, the Ca/P ratio is still relatively high, whereas at higher concentrations up to 2 M, the value gradually decreases toward the ideal hydroxyapatite ratio of 1.67. This indicates that higher H_3PO_4 concentrations provide more phosphate ions in the solution, making it easier for them to react with calcium ions. As a result, a phase richer in phosphate than calcium is formed. Therefore, the Ca/P ratio tends to decrease with increasing amounts of PO_4^{3-} ions. These findings are consistent with the literature, which states that the Ca/P ratio is strongly influenced by the balance of Ca^{2+} and PO_4^{3-} ions during the synthesis process, making precursor concentration control an important factor in obtaining hydroxyapatite with the desired composition [15].

3.3 XRD Analysis

X-ray diffraction (XRD) analysis was performed to identify the crystal structure and phases present in the synthesized samples. This method provides information about the atomic arrangement and the degree of order within the material. The resulting diffraction pattern exhibits characteristic features of each crystalline phase. In addition, this analysis can be used to determine the sample's crystallinity level. The XRD results were further analyzed to support the understanding of the properties and quality of the synthesized material.

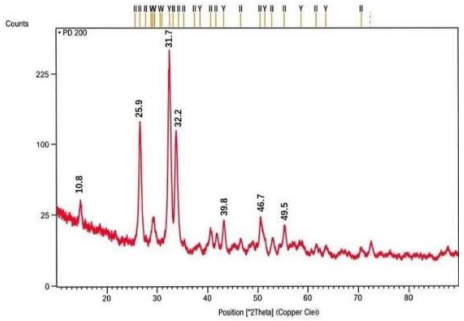

Figure 6. Hasil Uji XRD (*X-Ray Diffraction*) pada Hidroksiapatit

Based on Figure 6, the diffraction pattern shows several peaks at 2θ angles of approximately 10.8°; 25.9°; 31.7°; 32.2°; 39.8°; 46.7°; and 49.5°. The peaks in the range of 25.9° to 49.5° correspond to the characteristic pattern of hydroxyapatite, as per the JCPDS standard No. 09-0432. The highest intensity is observed in the 31–33° range, indicating the formation of a crystalline hydroxyapatite phase. Meanwhile, the low-angle peak at around 10.8° is likely associated with a minor phase or slight structural disorder. The relatively sharp diffraction peaks indicate that the material possesses a good degree of crystallinity. In addition, no other significant peaks besides hydroxyapatite are detected, suggesting that the formed phase is predominantly hydroxyapatite. Furthermore, the obtained crystal size falls within the nanocrystalline domain, confirming a structure within the permissible limit of <100 nm [16].

Table 4. Results of Crystal Analysis

Peak	2θ	FWHM	Crystal Size (nm)	Average Crystal Size (nm)
1	25.9	0.60	14.60	14.62
2	31.7	0.50	16.60	
3	32.2	0.50	16.30	
4	39.8	0.55	14.50	
5	46.7	0.60	13.30	
6	49.5	0.65	12.40	

Based on Table 4, the average crystal size of the synthesized hydroxyapatite is approximately 14.62 nm, indicating a nanoscale size. This value is obtained from relatively sharp FWHM values in the range of 0.50–0.65, with the largest crystal size of 16.60 nm observed at 2θ = 31.7°. The small particle size increases the material's specific surface area, enhancing interaction between hydroxyapatite and the biological environment. This condition enhances the material's bioactivity and facilitates the adhesion and proliferation of osteoblast cells. In addition, the particle size, which resembles that of natural bone minerals, plays an important role in supporting the bone tissue regeneration process [17].

Table 5. Results of Crystalline-Amorphous Fraction Analysis

Peak	2θ	Crystalline Fraction	Amorphous Fraction	%Crystallinity
1	25.9	30.5	98,79	81,23
2	31.7	115.2		
3	32.2	149.8		
4	39.8	31.7		
5	46.7	45.1		
6	49.5	55.6		

From the data presented in Table 5, the crystalline and amorphous fractions of the hydroxyapatite compound were identified. These parameters were then used to determine the degree of crystallinity using the following equation:

$$Crystallinity = \frac{crystalline\ area\ fraction}{crystalline\ area\ fraction + amorph\ fraction}\ x\ 100\%$$

Based on the calculation results, the degree of crystallinity obtained is 81.23%. This indicates that the crystal structure is well formed and highly ordered. Such structural regularity contributes to improved strength and stability of the material. Generally, a higher degree of crystallinity is associated with better material properties. Therefore, the synthesized hydroxyapatite exhibits good quality and is suitable for biomedical applications [18].

3.4 FTIR Analysis

Fourier Transform Infrared Spectroscopy (FTIR) analysis was conducted to identify the functional groups present in the synthesized samples. This method provides information about chemical bonds based on the absorption of infrared radiation at specific wavelengths. The resulting FTIR spectrum exhibits characteristic peaks corresponding to the functional groups in the material. By analyzing these absorption peaks, the chemical composition and molecular structure of the sample can be determined. The FTIR analysis results are used to support and confirm the identification the formed of material.

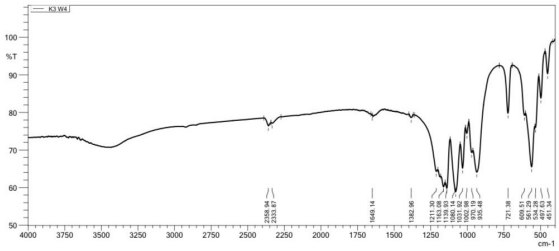

Figure 7. Results of FTIR Analysis on Hydroxyapatite

Based on Figure 7, absorption bands corresponding to phosphate groups (PO_4^{3-}) are detected in the regions of 1030–1100 cm^{-1}, 960 cm^{-1}, and 560–600 cm^{-1}, indicating the formation of hydroxyapatite. In addition, bands observed in the range of 1380-1470 cm^{-1} suggest the presence of carbonate groups (CO_3^{2-}) within the structure. The hydroxyl (OH^-) group is not significantly observed, possibly due to substitution processes or its low concentration. The sharp phosphate peaks indicate a high phosphate content and good crystallinity of the material. Overall, the FTIR results confirm the formation of hydroxyapatite, with a possible carbonate substitution in its structure [19].

3.5 Optimization of Ca/P Ratio Data Using Response Surface Methodology (RSM)

Optimization was performed to determine the optimal conditions for hydroxyapatite synthesis with a Ca/P ratio approaching 1.67. The variables analyzed in the Response Surface Methodology (RSM) include H_3PO_4 concentration (M) and heating time (hours). The method used was a Central Composite Design (CCD) with 9 experimental runs, and the response variable was the Ca/P ratio. The optimization results are presented in the following table.

Table 6. Experimental Factors and Ca/P Ratio Response

Run	Factor 1 H_3PO_4 Concentration (M)	Factor 2 Heating Time (hours)	Response Ca/P Ratio
1	0.5	1	2.8
2	1	1.5	2.1
3	1.5	2	1.71
4	1.5	2.5	1.6716
5	1.5	3	1.6638
6	2	1.5	1.687
7	2	2	1.6566
8	2	2.5	1.6782
9	2	3	1.77

Based on Table 6, H_3PO_4 concentration and heating time influence the Ca/P ratio of hydroxyapatite. At low concentrations (0.5–1 M), the ratio remains high, indicating that the conditions are not yet optimal. Increasing the concentration to 1.5–2 M results in a ratio closer to 1.67, suggesting that the balance between Ca^{2+} and PO_4^{3-} ions is being achieved. A heating time of 2–2.5 hours provides the best results. However, extending the time to 3 hours causes the ratio to deviate again from the optimum value.

Table 7. Comparison of RSM Models

Source	Sequential p-value	Adjusted R^2	Predicted R^2	
Linier	0,0080	0,7335	0,3217	
2R	0,0006	0,0742	0,9043	
Quadratic	**0,0014**	**0,9995**	**0,9963**	**Suggested**
Cubic				**Allowed**

Based on Table 8, a model equation was derived to predict the Ca/P ratio as a function of H_3PO_4 concentration and heating time. The most suitable model is the quadratic model, as the adjusted R^2 value of 0.9995 and the predicted R^2 value of 0.9963 are very close, indicating an excellent fit. The small difference between these two values reflects the model's high predictive capability. In addition, the p-value of 0.0014 (<0.05) indicates that the model is statistically significant. Therefore, the quadratic model is appropriate to represent the relationship between the process variables and the Ca/P ratio.

The relationship between H_3PO_4 concentration and heating time on the Ca/P ratio response is visualized in the form of contour plots and 3D surface plots as shown below:

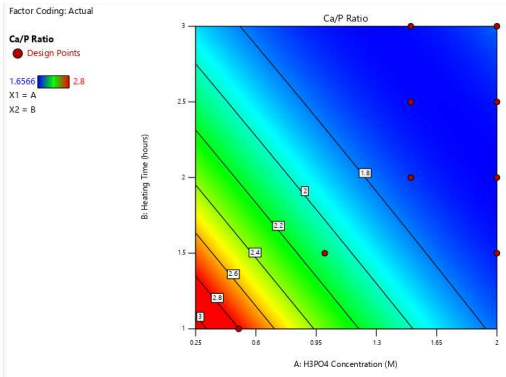

Figure 8. Contour Plot of H_3PO_4 Concentration (M) and Heating Time (hours) on Ca/P Ratio

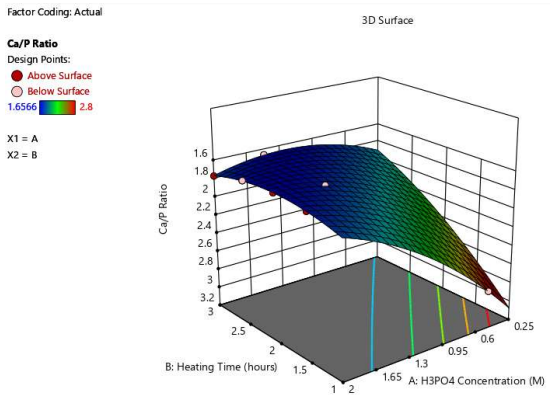

Figure 9. 3D Surface Plot of H_3PO_4 Concentration (M) and Heating Time (hours) on Ca/P Ratio

A contour plot is a two-dimensional representation of the response, presented using a predictive model for the Ca/P ratio, while a 3D surface plot shows its three-dimensional representation. Based on Figure 8 and Figure 9, the relationship between H_3PO_4 concentration (A) and heating time (B) on the resulting Ca/P ratio is illustrated, where the contour plot provides a two-dimensional visualization, and the 3D surface plot displays the response surface in three dimensions. From both graphs, it can be observed that both variables influence changes in the Ca/P ratio during the synthesis process. The highest Ca/P ratio, approximately 2.8, is obtained at low H_3PO_4 concentrations (around 0.25–0.6 M) and short heating times (around 1–1.5 hours), as indicated by the red region on the surface. In contrast, the lowest Ca/P ratio, approximately 1.6–1.8, is achieved at higher H_3PO_4 concentrations (up to 2 M) and longer heating times (up to 3 hours), as indicated by the blue region. In hydroxyapatite synthesis, variations in H_3PO_4 concentration show that the final Ca/P ratio tends to decrease with increasing H_3PO_4 concentration and heating time. This trend is also reflected in the color transition on the surface plot from red–yellow to green–blue. Red to yellow regions indicate higher Ca/P ratios, while green to blue regions indicate lower Ca/P ratios, suggesting that increasing H_3PO_4 concentration and heating time enhances the phosphorus content relative to calcium. Thus, it can be concluded that increasing H_3PO_4 concentration and heating time tends to decrease the Ca/P ratio. Therefore, to obtain a Ca/P ratio close to the stoichiometric value of hydroxyapatite (1.67), a combination of higher H_3PO_4 concentration and longer heating time is required [20].

4. CONCLUSION

The synthesis of hydroxyapatite (HA) from snail shells (*Pila ampullacea*) using the precipitation method has been successfully carried out. Variations in H_3PO_4 concentration and heating time significantly affect the Ca/P ratio, with higher values of both parameters decreasing it toward the stoichiometric value of hydroxyapatite (1.67). Optimum conditions were obtained at approximately 1.5–2 M H_3PO_4 and a heating time of 2–2.5 hours. Characterization results using SEM-EDX show a porous and agglomerated surface morphology, while XRD analysis confirms the formation of a crystalline hydroxyapatite phase with a crystallinity degree of 81.23% and an average crystal size of 14.62 nm. FTIR analysis also supports the presence of phosphate groups as the main component of hydroxyapatite. Overall, this study demonstrates that snail shells have strong potential as an effective and sustainable alternative calcium source for the synthesis of hydroxyapatite in biomaterial applications.

REFERENCE

[1] F. Behmagam, S. M. Dhiaa & A. H. A. Hussein, 'Hydroxyapatite–Polymer Nanocomposites for Drug Delivery Applications: A Mini Review', *European Journal of Medicinal Chemistry Reports*, 1(1), 1-13, 2024.

[2] A. Iatsenko, O. Syech, A. Nikolenko & S. Stelmakh, 'Structure Investigation Of Highly Porous Bioceramics Based On Biogenic Hydroxyapatite With Graphene Oxide Coating', *Journal Results In Surfaces And Interfaces,* 2(1), 19-38, 2024.

[3] M. S. F. Hussin, H. Z. Abdullah, M. I. Idris & M. A. A. Wahap,'Extraction Of Natural Hydroxyapatite For Biomedical Applications A Review', *Journal Heliyon,* 8(1), 10-19, 2022.

[4] S. Patil, S. Thanikodi, S. Palaniyappan, J Giri, A. O Hourani & M. Azizi,' Sustainable synthesis of marine-derived hydroxyapatite for biomedical applications: a systematic review on extraction methods and bioactivity', *Advanced Manufacturing:Polymer & Composite Science*, 11(1), 1-30, 2025.

[5] H. Y. Ahmed, N. Safwat, R. Shehata, & E. H. Althubaiti,' Synthesis of Natural Nano-Hydroxyapatite from Snail Shells and Its Biological Activity: Antimicrobial, Antibiofilm, and Biocompatibility', *Journal Membraness,* 12(4), 1-16, 2022.

[6] Z. Kareem & E. Eyiler,'Synthesis Of Hydroxyapatite From Eggshells Via Wet Chemical Precipitation: A Review', *RSC Advances,* 14(1), 21439–21452, 2024.

[7] W. Chaiyacet, R. Junggoth, T. Donprajum, S. Yasaka, R. Chaiyacet & E. Kanchanatip, 'Microwave-assisted hydrothermal synthesis of hydroxyapatite from fermented fish by-product for removal of lead from contaminated water', *Beni-Suef University Journal of Basic and Applied Sciences,*14(116), 1-22, 2025.

[8] H. Atta, K. R. Mahmoud, E. I. Salim, E. Elmohsnawy & A. El-Shaer, 'Correlation Between Positron Annihilation Lifetime and Photoluminescence Measurements for Calcined Hydroxyapatite', *Scientific Reports,* 14(1), 10370, 2024.

[9] N. Keanjun, T. Rattanawongwiboon, P. Sricharoen & S. Laksee, 'Ultrasound-Assisted Formation of Composite Materials from Fish Scale Waste Hydroxyapatite in the Presence of Gamma-Irradiated Chitosan for The Removal of Malachite Green', *RSC Advances*, 14(1), 29737–29747, 2024.

[10] S. Balhuc, R. Campian, A. Labunet, M. Negucioiu S. Buduru & A. Kui, 'Dental Applications of Systems Based on Hydroxyapatite Nanoparticles an Evidence-Based Update', *Journal Crystals,* 11(1), 674, 2021.

[11] M. U. Munir, S. Salman, A. Ihsan & T. Elsaman,' Synthesis, Characterization, Functionalization and Bio-Applications of Hydroxyapatite Nanomaterials: An Overview', *International Journal of Nanomedicine*, 17(1),1903-1925, 2022.

[12] N. Tian, G. Zhang, P. Yan, P. Li, Z. Feng & X. Wang, 'Simulation and Experimental Study on the Effect of Superheat on Solidification Microstructure Evolution of Billet in Continuous Casting', *Materials*, 17(3), 1-14, 2024.

[13] W. Khoo, F. M. Nor, H. Ardhyananta & D. Kurniawan, 'Preparation of Natural Hydroxyapatite from Bovine Bone Based on Calcination at Different Temperatures', *Procedia Manufacturing*, 2, 98-102. 2015.

[14] M. Trzaskowska, V. Vivcharenko & A. Przekora, 'The Impact of Hydroxyapatite Sintering Temperature on Its Microstructural, Mechanical, and Biological Properties', *International Journal of Molecular Sciences*, 24(6), 1-21. 2023.

[15] S. V. Dorozhkin,'Calcium orthophosphates ($CaPO_4$) Occurrence and properties', *Progress in Biomaterials*,5(1), 9–70, 2016.

[16] M. Kawsar, M. S. Hossain, S. Tabassum, D. Islam, N. M. Bahadur & S. Ahmed, 'Crystal Structure Modification of Nanohydroxyapatite Using Organic Modifiers and Hydrothermal Technique', *RSC Advances*, 14(1), 29665-29674, 2024.

[17] J. Venkatesan, R. V. Anchan, S. S. Murugan, S. Anil & S. K. Kim, 'Natural Hydroxyapatite-Based Nanobiocomposites and Their Biomaterials-To-Cell Interaction for Bone Tissue Engineering', *Discover Nano*, 19(1), 169, 2024.

[18] S. L. Bee, S. N. F. M. Noor, A. U Hamid & Z. A. A. Hamid, 'Effect of calcination temperature on the physicochemical properties of natural hydroxyapatite derived from Catla fish bone', *Journal of Physics: Conference Series*, 2907(1), 1-7, 2024.

[19] S. C. Wu, H. C. Hsu, W. H. Wu & W. F. Ho, 'Enhancing Bioactivity and Mechanical Properties of Nano-Hydroxyapatite Derived from Oyster Shells through Hydrothermal Synthesis', *Nanomaterials*, 14(15), 1-16, 2024.

[20] E. A. A. Aal, D. E. Sayed & H. M. A. Ghafar, 'Hydrothermally synthesized nanoscale carbonated hydroxyapatite with calcium carbonates derived from green mussel shell wastes', *Discover Applied Sciences*, 6(143), 2024.